JOURNAL OF MATERIALS SCIENCE 15 (1980) 230–236

Flow and fracture of a Ni-Fe metallic glass

L. A. DAVIS, Y. T. YEOW
Corporate Development Center, Allied Chemical Corporation, Morristown, NJ 07960, USA

When brittle failure modes are bypassed, sheet tensile specimens of $Ni_{49}Fe_{29}P_{14}B_6Si_2$ glass exhibit abrupt shear failures, coincident with yielding; at low to intermediate temperatures no reduction of area is evident in the narrow shear zone. At higher temperatures (up to 0.87 T_g, where T_g is the glass transition temperature) plastic flow at ordinary strain rates is different only in that it is less localized, i.e. yielding induces readily evident necking through the thickness of the sheet; failure still generally occurs by shear rupture through the neck. In the low temperature regime, the yield stress (σ_Y) decreases slowly with increasing temperature; it varies from 3.04 to 1.96 GPa between 77 and 568 K ($T/T_g \simeq 0.82$). At higher temperatures, where necking is observed, σ_Y decreases rapidly, apparently approaching zero near T_g ($\sim$694 K).

The oblique shear zones which are generated by yielding apparently follow (or are close to) directions of zero extension (i.e. pure shear) in the sheet specimens. For $Ni_{49}Fe_{29}P_{14}B_6Si_2$ the angle between the normal to the shear "plane" and the tensile axis averages $\sim 37°$, only a few degrees larger than the expected value. This small variation may derive from the dynamics of the yielding process.

Oblique necking and shear through the neck occur during tensile deformation of crystalline material only when the sample is in sheet form; also the shear localization zone lies parallel to the thickness vector of the sheet. Metallic glasses are unique in that (1) the shear zone in low aspect ratio sheets is sometimes oblique to the thickness vector (as well as the width vector) and (2) shear yielding also occurs along directions of zero extension in radially symmetric (as opposed to sheet) gauge section specimens.

1. Introduction

Metallic glass strips typically fail by tearing, [1, 2] a common mode of failure for thin sheets of high strength materials [3]. If grip and edge constraints can be suppressed, tearing can be avoided and shear failure occurs following plastic instability [4]. At ambient temperature and below, such failures occur with catastrophic rapidity coincident with instability. According to the investigations of $Pd_{80}Si_{20}$ by Masumoto and Maddin [5] and Megusar *et al.* [6], at somewhat elevated temperatures failure is preceded by pronounced localized reduction of area, i.e. necking. The transition between these two regimes, i.e. rapid failure and "delayed" failure, occurs rather abruptly in the vicinity of $T/T_g \geqslant 0.7$, where T_g is the glass transition temperature. On the high side of the transition the stress for plastic flow drops much more rapidly than at lower temperatures and becomes more strain rate sensitive [6]. Argon [7] has presented a phenomenological theory of the plastic flow of metallic glasses and applied it to the temperature and strain-rate dependence of flow in $Pd_{80}Si_{20}$ glass.

The low temperature ($T \ll T_g$) deformation and fracture modes of metallic glasses appear to be independent of chemical composition. It seems likely that their intermediate temperature behaviours will be rather similar also. To probe this point, we present here, for comparison with results reported for $Pd_{80}Si_{20}$ [2, 6] and $Pd_{77.5}Cu_6Si_{16.5}$ [8], an investigation of the temperature dependence of deformation and fracture of glassy $Ni_{49}Fe_{29}P_{14}B_6Si_2$ (METGLAS*

* Registered trade mark.

 0022–2461/80/010230–07$02.70/0

2826B). Particular emphasis is placed on a consideration of the subtleties of the plastic instability event.

2. Experimental procedure

The samples of $Ni_{49}Fe_{29}P_{14}B_6Si_2$ glass examined were obtained from the same continuous length of ribbon used for previous investigations of fracture toughness [9, 10], fatigue behaviour [11] and ambient temperature strength [4]. In the as-cast condition, the ribbon was ~ 75 to 80 μm thick and ~ 1 mm wide. To eliminate grip constraints, specimens with a reduced area gauge section ~ 0.22 to 0.64 mm wide by ~ 2 mm long were prepared by hand polishing. A single specimen of $Ni_{69}Cr_6Fe_3B_{14}Si_8$ glass with a nominally square gauge section was also tested. The specimens were tested in a table model Instron at an extension rate of $\sim 2.1 \times 10^{-3}$ mm sec^{-1}. Tests were conducted between ambient and liquid N_2 temperatures utilizing the Instron Temperature Chamber with boiling liquid N_2 vapour blowing through the chamber as the coolant. For tests at 77 K, a small polyethylene cup was affixed to the Instron cross-head around the grips and specimen, and filled with liquid N_2, completely immersing the specimen.

For higher temperature tests, a different arrangement was employed. A cage was constructed which allowed the specimen to be situated well below the cross-head of the machine. A stainless steel pot encased in a heating mantle and attached to a hand-operated jack, was filled with silicone oil and placed below the base of the cage. A Plexiglas hood was constructed to enclose the entire load frame of the Instron and the fumes from the hot oil were exhausted through a blower to an adajacent laboratory hood. For tensile testing the oil was pre-heated to the desired test temperature, the pot was raised to immerse the cage and 2 to 4 min were allowed for the sample and fixtures to equilibrate with the stirred bath before testing. The temperature was monitored (also for the low temperature tests) by a thermocouple affixed to the lower grip, in close proximity to the specimen, and was constant to within $\sim \frac{1}{2}$° C during the test. Using this oil immersion procedure one minimizes exposure of the specimen to high temperature prior to testing and, hence, minimizes the problem of annealing induced embrittlement [12, 13], which favours pre-yield fracture.

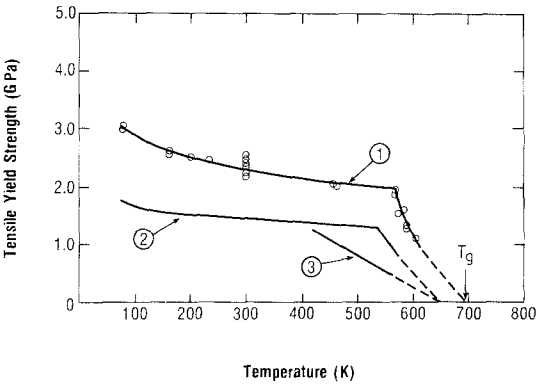

Figure 1 Tensile yield strength versus temperature: curve 1 for $Ni_{49}Fe_{29}P_{14}B_6Si_2$ glass; curve 2 for $Pd_{77.5}Cu_6Si_{16.5}$ glass from Pampillo and Chen [8]; curve 3 for $Pd_{80}Si_{20}$ glass from Megusar *et al.* [6]. The solid portion of each curve covers the range of the measured experimental data.

The highest test temperature employed was $\simeq 332$° C; slightly above this temperature the oil decomposes rapidly. Higher temperatures may be achieved using a molten salt bath, but, for the present, we have chosen to forego such experiments.

3. Results

3.1. Yield stress

The yield stresses of glassy $Ni_{49}Fe_{29}P_{14}B_6Si_2$ specimens, measured over the temperature range of 77 to 605 K are summarized in Table I and Fig. 1.† The values at 295 K, while not previously reported individually, were the basis of an earlier report of the (average) ambient temperature strength [4]. For specimens tested at 573 K and above, the load elongation curves exhibit a load maximum and subsequent modest load drop before failure. For these specimens, the yield stress (σ_y) is calculated using the maximum load and the initial cross-sectional area of the specimen. At temperatures $\leqslant 472$ K, the load elongation curves are essentially linear to failure. Plastic instability, i.e. yielding, is indicated by the oblique (slanting across the width) failure mode of the specimen. The yield stress is given, again, by the load maximum and initial area. At temperatures near the

† For the sake of simplicity, we have chosen to report tensile stresses. The maximum shear stresses seen by the specimens are, of course, given by $\tau = 0.5\ \sigma_y$. In the fracture zone the shear stress is slightly less. When $\beta = 0$ and $\theta = 36.7°$, $\tau_y \simeq 0.48\ \sigma_y$; when $\beta = 19.5$ and $\theta = 38.9°$, $\tau_y \simeq 0.49\ \sigma_y$, assuming that the first infinitesimal increment of shear occurs in the direction of maximum shear stress in the shear zone.

TABLE I Yield stresses and fracture surface orientation for $Ni_{49}Fe_{29}P_{14}B_6Si_2$ glass samples

Sample no.	T (K)	σ_y (GPa)	α (°)	β (°)	θ (°)	W (mm)
86	77	3.02	53.0	18.4	39.5	0.279
87	77	3.07	54.0	6.0	36.3	0.253
84	159	2.58	53.7	0	36.3	0.257
85	159	2.63	53.0	7.5	37.4	0.235
25	199	2.54	53.5	10.0	37.3	0.218
24	233	2.47	53.5	1.5	36.5	0.243
8	295	2.50	53.4	0	36.6	0.545
9	295	2.44	53.0	0	37.0	0.563
10	295	2.21	53.5	0	36.5	0.599
13	295	2.38	53.1	0	36.9	0.642
15	295	2.41	53.2	0	36.8	0.284
16	295	2.30	52.5	0	37.5	0.264
17	295	2.42	53.5	0	36.5	0.625
91	456	2.10	54.0	19.5	38.9	0.225
90	462	2.03	54.1	0	35.9	0.237
93	565	1.88	*			0.229
97	568	1.97	53.5	4.0	36.6	0.246
96	573	1.55	*			0.226
94	583	1.62	*			0.226
95	588	1.30	*			0.226
98	588	1.35	*			0.269
99	605	1.13	*			0.226

* Specimen too distorted to measure angles.

knee of the curve (Fig. 1), linear (568 K) or load drop (565 K) behaviour can occur.

As is evident from Fig. 1, σ_y decreases moderately, from ~3.04 to 1.96 GPa, when temperature is increased from 77 to 568 K; it falls precipitously as T is further increased (to ~1.13 GPa at 605 K) approaching near zero, apparently, at the glass transition of the alloy (694 K, as determined in a differential scanning calorimeter at a heating rate of 20° C min^{-1}).

3.2. Instability and fracture

At low to medium temperatures, metallic glasses fail at yielding by shear rupture through a prior plastic shear zone. Hence, the orientation of the fracture surface defines the zone of unstable plastic flow. Table I indicates the angles α and β, as defined in Fig. 2, which characterize the orientation of the (nominally flat) fracture surface. For the wider specimens ($w > 0.54$ mm, $w/t > 7$; where w = width and t = thickness), the surface was always parallel to the thickness vector **t** ($\beta = 0$). For the narrower specimens ($w < 0.28$ mm, $w/t < 3.7$), the surface was often (7 of 12) slightly inclined to **t** ($\beta \neq 0$). For the case $\beta = 0°$, the average value of α was 53.3°. In this case, the angle between the tensile axis (T) and the normal to the fracture plane (N) is 36.7°. For the $\beta \neq 0$ specimens, the angle between T and N (defined as θ, not shown in Fig. 2) is given by $\cos\theta = [1 + \tan^2\gamma + \tan^2\beta]^{-1/2}$, where $\gamma = 90 - \alpha$. Inspection of Table I indicates that θ changes only slightly when β approaches 20°.

For temperatures > 568 K, the onset of necking is quite gradual. As the neck intensifies, simultaneous shear proceeds through it, parallel, essen-

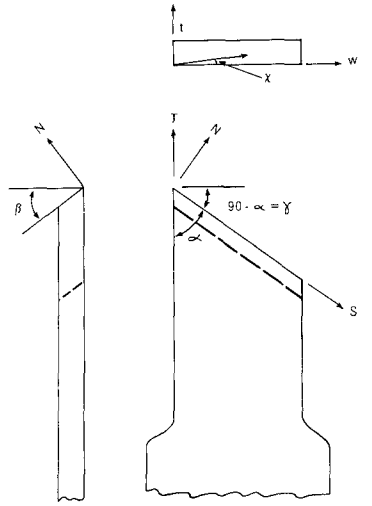

Figure 2 Samples which fall in the low temperature regime ($T/T_g \lesssim 0.8$) exhibit a fracture surface orientation defined by the angles α and β, shown in the front and side views of the figure. Vector **T** defines the tensile direction and **N** the normal to the fracture surface; **t** and **w** represent the thickness and width vectors of the sample.

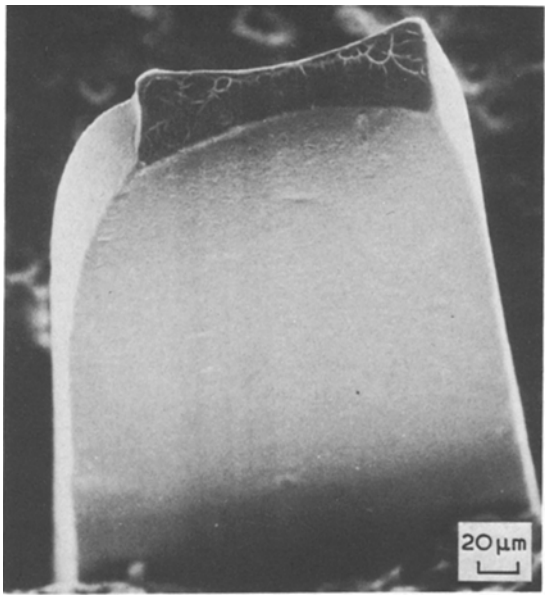

Figure 3 A view of the necking and shear distortion which occur in a sample (no. 94) tested at 583 K [scanning electron micrograph (SEM)].

tially, to the broad faces of the specimen. Before the neck is sufficiently pronounced to measure its inclination (α and β), the distortion of the specimen (see Fig. 3) occasioned by the shear displacement makes such a measurement unreliable.

Figs. 4a to c exhibit the fracture surfaces of specimens tested at 77 K (no. 87), 456 K (no. 91) and 583 K (no. 94). The lower temperature specimens (4a and b) fail with no apparent reduction in area. At higher temperatures, as evidenced in Fig. 4c, pronounced area reduction occurs (the three specimens had approximately the same initial cross-sectional area); the specimen in Fig. 4c failed by tearing through the neck (shear displacement in the direction **t** of Fig. 2). At 456 K, the localized shear displacement prior to failure is clearly evidenced by the featureless zone at the right-hand edge of the micrograph, (Fig. 4b; the markings covering the remainder of the surface are known as vein markings) shear having occurred in the direction **S** (approx.) shown in Fig. 2. At 77 K, such a zone also occurs ($\sim \frac{1}{3}$ as wide), but the veins are too fine to delineate it at the magnification shown. In general, the micrographs shown are typical in that the vein markings become progressively finer as the test temperature is reduced. The broader, arrow like markings evident in Fig. 4a indicate undulations in the fracture surface and appear to be characteristic of fractures where the fracture zone is not parallel to the thickness vector (i.e. $\beta \neq 0$). Similar markings are evident in Fig. 4b.

For specimens with $\beta = 0$, the direction of shear displacement is parallel to the broad faces of the specimen in the direction **S** in Fig. 2, which is the direction of maximum shear stress. When $\beta \neq 0$ the maximum shear stress direction and the width vector are oblique to one another; as seen on a horizontal projection of the fracture surface, (topview, Fig. 2; the manner in which Figs. 4a to c are viewed) the angle between them is given by $\chi = \arctan(\tan\beta/\tan 90 - \alpha)$. Given an oblique shear direction, featureless zones meeting at a corner, indicative of prior shear, should appear along both an edge and face of the specimen. For small χ ($< 10°$) this was not observed. For larger χ a "face" featureless zone was sometimes observed, (e.g. Fig. 4b at the top) but it was not as wide as would be expected from the value of χ. In general, even when the prior shear zone is oblique to width and thickness vectors ($\beta \neq 0$), shear displacements highly oblique to the broad faces of the specimen, in the direction of maximum shear stress, do not occur, presumably because they are suppressed by the bending moments which would be attendant with such displacements.

Any constraint associated with a ribbon shaped gauge section is removed, obviously, when the specimen is nearly square in cross-section. Fig. 5 shows the fracture surface of such a specimen of glassy $Ni_{69}Cr_6Fe_3B_{14}Si_8$ tested at 295 K (σ_y = 2.78 GPa) for which $\alpha = 55°, \beta = 11°$ and $\theta = 36°$. In this case $\chi \simeq 15.5°$, but the shear displacement is again nearly parallel to the (original) broad face of the specimen.

4. Discussion

4.1. Yield stress

The variation of σ_y with T for $Ni_{49}Fe_{29}P_{14}B_6Si_2$ glass is compared with that for $Pd_{77.5}Cu_6Si_{16.5}$ [8] and $Pd_{80}Si_{20}$ [6] in Fig. 1. On a relative scale (σ/σ_{0K} versus T/T_g), the behaviours of the first two alloys appear to be essentially identical. For $Pd_{80}Si_{20}$, the break in σ_y versus T occurs at a somewhat lower temperature relative to T_g. This suggests, perhaps, that the structure of a binary alloy is somewhat less stress stable than those of multicomponent alloys. On the other hand, the load–elongation curves for $Pd_{80}Si_{20}$ reported by Masumoto and Maddin [2] suggests a "break" temperature between ~473 and ~523 K (a load drop occurs at 523 K, but not at 473 K). This

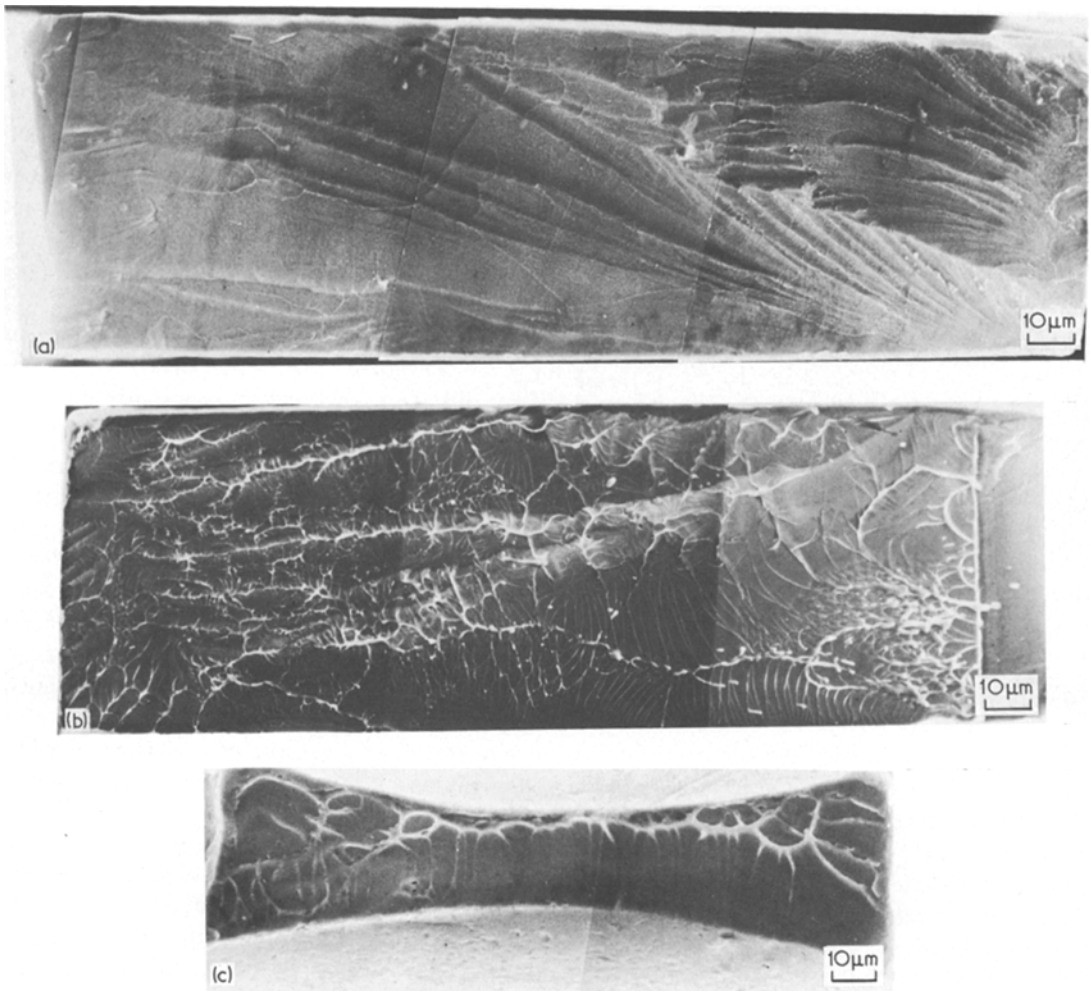

Figure 4 (a) Fracture surface of a $Ni_{49}Fe_{29}P_{14}B_6Si_2$ specimen which yielded and failed at 77 K. The specimen is viewed approximately along the tensile direction; surface slopes down from left to right. The arrow-like surface markings appear to be typical of specimens for which $\beta \neq 0$. The typical vein pattern observed on shear rupture failures of metallic glass is present, but it is too fine to be clearly seen at the magnification shown (SEM). (b) Fracture surface of a Ni_{49} specimen which yielded and failed at 456 K. The surface slopes as in (a). Note the larger scale of the vein pattern observed at higher testing temperature (SEM). (c) Fracture surface of a Ni_{49} specimen which yielded and failed at 583 K (same specimen as in Fig. 3). The direction of view is approximately along the tensile axis; the surface slopes down from right to left. In this case, failure was preceded by large scale necking and occured by tearing through the neck. This specimen originally had approximately the same gauge dimensions as those of (a) and (b) (SEM).

appears somewhat more consistent with the behaviours of the Pd–Cu–Si and Ni alloys than the results presented by Megusar *et al.* [6].

As the σ_y versus T behaviour observed for the Ni alloy is nominally similar to that for the Pd alloys, it would probably be well described by the formalism developed by Argon [7] and applied to the Pd alloys. The formalism cited employs relationships characteristic of dislocation mechanics and assumes that the "flow" volume is disc shaped at low temperature and spherical, hence less localized, at higher temperature. With this and other distinctions, one thereby generates two branches of the σ_y versus T behaviour with very different slopes. While this approach is instructive, it must be employed in a curve fitting rather than a predictive capacity. For the present purposes, it is simply sufficient to note that it could be used to fit the σ_y versus T behaviours of the Ni alloy.

4.2. Instability and fracture

The occurrence of oblique necking and shear instability in sheet-shaped specimens is attributed to geometrical constraint, i.e. thinning of the

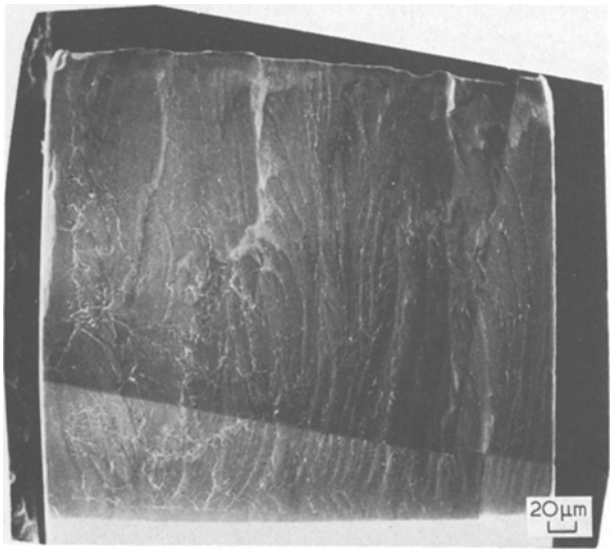

Figure 5 Fracture surface of $Ni_{69}Cr_6Fe_3B_{14}Si_8$ specimen tested at 295 K. The surface slopes down from top to bottom. A vein pattern typical of shear rupture failure appears on a rather fine scale. The significant feature of this failure is that it occurs along (or near) a direction of zero extension even though the specimen is nominally square in cross-section. A ductile polycrystalline rod would neck normal to the tensile axis (SEM).

specimen is suppressed in the width direction. Hence, the neck is expected to follow a direction of zero extension in the material; the tensile stress resolved parallel to such a direction is equal to one half that resolved perpendicular to it [14–18]. In the plane of the sheet, the direction so defined is characterized (Fig. 2) by the angle $\alpha = 54.7^\circ$ and is identically a direction of pure shear in the material. One may locate directions of pure shear more generally by noting that they lie in planes whose normals make angles (θ_1) of 35.3° (in the loaded state) with the tensile axis. According to Argon, when the yield stress is a large fraction of Young's modulus (E) there will be a slight difference between the angles in the loaded and unloaded states; in the unloaded state θ is given by

$$(90^\circ - \theta) = \cos^{-1}\{\sqrt{(\tfrac{1}{3})}[1 - \sigma_y/E(1+\nu)]\}$$

where ν = Poisson's ratio.* For METGLAS 2826B, with $\sigma/E \simeq 0.0159$ and $\nu = 0.37$, θ is expected to be $\sim 34.4^\circ$.

For thin sheets of crystalline materials (low σ/E) θ is rarely precisely 35.3°. Typically it is less (28 to 32°; see e.g. [17, 18]) and the difference has been attributed to the existence of a texture in the sheet [14] and to the development of bi-axial stresses due to diffuse thinning of the sheet in the width direction prior to intense oblique necking and shear localization [17, 18]. Inspection of Table I, indicates that θ for METGLAS 2826B also differs from the expected value, although in this case, it is a few degrees larger (36.3 to 39.5°). Megusar *et al.* observed $\theta \simeq 39^\circ$ for $Pd_{80}Si_{20}$. One could account for the observed angle as deviation from shear yielding at 45°, if, as for organic glasses such as polystyrene, the stresses for plastic flow in metallic glasses were highly normal stress dependent. For the one alloy ($Pd_{77.5}Cu_6Si_{16.5}$) for which the pressure dependence of flow was examined, $d\sigma/dP$ was found to be small [19]. This is not too surprising, given that glassy alloys are essentially close packed materials (the difference in density between identical glassy and crystalline compositions is only 1 to 2%). Hence, one can discount the possibility that the observed θ represents a normal stress induced variation of 45° shear yielding.

As an alternative explanation, one may speculate that the values of θ reflect the response of the material to the dynamics of yielding. At low to intermediate temperatures, yielding of metallic glasses is accompanied by an abrupt drop of load. Hence, at the instant that yielding initiates the material undergoes a rapid lateral elastic expansion. Accordingly, the "dynamic" direction of zero extension will lie at a larger angle θ, where the parallel resolved stress is slightly less than one half the perpendicular resolved stress.

The inclination of the fracture surface discussed

* Argon's [16] treatment contains a printing error [argument of arc cos is given as $\sqrt{(2/3)}$] from which one would deduce that θ in the unloaded state is greater than that in the loaded state, rather than vice versa. This error went undetected in a previous discussion of the ambient temperature properties of METGLAS 2826B [4].

above is not to be confused with that observed when the specimen fails by tearing through the thickness (prior to general yielding). In this case, one would expect the failure surface to be inclined (θ) at $\sim 45^\circ$ to the tensile axis (with $\alpha = 90^\circ$), but θ is often found to be $\sim 40^\circ$. *In situ* microscopic observations of the tearing fractures of specimens [10] have suggested that, in this case, the observed surface inclination results due to severe buckling of the specimen near the tip of the shear crack.

As is suggested above, necking and shear localization along directions of (near) zero extension during tensile deformation only occur in sheet-shaped specimens of crystalline materials. In square or round cross-section tensile specimens, necking occurs normal to the tensile axis. In metallic glasses, such is not the case. This is suggested by the failures with $\beta \neq 0$ observed for low aspect ratio sheets and is firmly evidenced by the experiment cited above for the nominally square gauged Ni_{69} alloy specimen, which failed with $\theta = 36^\circ$ †. While, at high temperatures, normal necking would probably occur in glassy alloys due to multiple shear events along directions of zero extension, at room temperature the first such event leads to catastrophic failure. In this sense, metallic glasses bear a strong resemblance to single crystals with a few highly preferred slip systems.

According to Chakrabarti and Spretnak [17, 18], in a material capable of work hardening, "diffuse" necking will always precede shear localization in the oblique neck. In a non-hardening material, such as a metallic glass, necking and shear localization will occur simultaneously. Whether or not one can distinguish "necking" depends on the rate at which the shear instability propagates. At low to intermediate temperatures this occurs with catastrophic rapidity in METGLAS 2826B and the "neck" is imperceptible.

At higher temperatures, thermally activated, stress driven atomic motion comes into play, accounting for the sharp break in the σ_y versus T behaviour. Thermal motion will, obviously, have less impact at higher strain rates and, hence, both the "break" temperature and the flow stress at a given temperature will increase with strain rate, as observed by Megusar *et al.* [6]. As suggested by Argon [7] this effect leads to "strain rate hardening" which provides for a relative stabilization of the neck at high temperature, even though the material does not strain harden.

5. Conclusion

The yield stress of glassy $Ni_{49}Fe_{29}P_{14}B_6Si_2$ decreases moderately with increasing temperature in the range up to $T/T_g \sim 0.8$; at higher temperatures σ_y falls precipitously, apparently approaching near zero at T_g. Coincident with the break in the σ_y versus T behaviour, the failure characteristics of the material change. Below $T/T_g \sim 0.8$ the specimen exhibits oblique shear failure with no apparent reduction of area; at high temperatures pronounced oblique necking is observed prior to shear rupture failure through the neck. As in the case of thin sheets of crystalline materials, metallic glass sheets exhibit failure by shear localization along (or close to) directions of pure shear (zero extension). Pure shear failures also occur in square or circular cross-section metallic glass samples, contrary to the case for ductile crystalline materials where failure would follow necking normal to the tensile axis.

References

1. H. J. LEAMY, H. S. CHEN and T. T. WANG, *Met. Trans.* **3** (1972) 699.
2. T. MASUMOTO and R. MADDIN, *Acta Met.* **19** (1971) 725.
3. A. S. TETELMAN and A. J. MCEVILY, Jr., "Fracture of Structural Materials", (John Wiley, New York, 1966) p. 94.
4. L. A. DAVIS, *Scripta Met.* **9** (1975) 339.
5. T. MASUMOTO and R. MADDIN, *Mater. Sci. Eng.* **19** (1975) 1.
6. J. MEGUSAR, A. S. ARGON and N. J. GRANT, *Mater. Sci. Eng.* **38** (1979) 63.
7. A. S. ARGON, *Acta Met.* **27** (1979) 47.
8. C. A. PAMPILLO and H. S. CHEN, *Mater. Sci. Eng.* **13** (1974) 181.
9. L. A. DAVIS, *J. Mater. Sci.* **10** (1975) 1557.
10. L. A. DAVIS, *Met. Trans. A* **10A** (1979) 235.
11. L. A. DAVIS, *J. Mater. Sci.* **11** (1976) 711.
12. F. E. LUBORSKY, J. J. BECKER and R. O. MCCARY, *IEEE Trans.* **MAG-11** (1975) 1644.
13. L. A. DAVIS, R. RAY, C.-P. CHOU and R. C. O'HANDLEY, *Scripta Met.* **10** (1976) 541.
14. R. HILL, "The Mathematical Theory of Plasticity", (Oxford University Press, London, 1967) p. 300.
15. A. NADAI, "Theory of Flow and Fracture of Solids", (McGraw-Hill, New York, 1950) p. 319.
16. A. S. ARGON, in "The Inhomogeneity of Plastic Deformation", (American Society for Metals, Metals Park, Ohio, 1973) p. 161.
17. A. K. CHAKRABARTI and J. W. SPRETNAK, *Met. Trans. A* **6A** (1975) 733.
18. *Idem, ibid.* **6A** (1975) 737.
19. L. A. DAVIS and S. KAVESH, *J. Mater. Sci.* **10** (1975) 453.

Received 24 May and accepted 28 June 1979.

† In retrospect, it is apparent that $Pd_{77.5}Cu_6Si_{16.5}$ wires probably fail with $\theta \sim 40^\circ$ [19]. It is difficult to establish θ precisely because the specimens in question were locally distorted by the shear displacement preceding failure.